



Influences of the diameter of the balance hole on the flow characteristics in the hub cavity of the centrifugal pump^{*}

Wei Dong¹, Wu-li Chu², Zai-lun Liu³

1. *College of Water Resources and Architectural Engineering, Northwest A&F University, Yangling 712100, China*

2. *School of Power and Energy, Northwestern Polytechnical University, Xi'an 710129, China*

3. *College of Energy and Power Engineering, Lanzhou University of Technology, Lanzhou 730050, China*

(Received January 18, 2017, Revised March 22, 2019, Accepted March 24, 2019, Published online April 12, 2019)

©China Ship Scientific Research Center 2019

Abstract: The diameter of the impeller balance hole in a centrifugal pump is closely related to axial force. Thus, to select the appropriate diameter of a balance hole is crucial for balancing the axial force of the centrifugal pump. After the validation of the CFD method and the grids independence study, the characteristics of flow in the hub cavity have been analyzed in 4 cases with different diameters of balance holes. The leakage rate of the liquid in the hub cavity of the centrifugal pump is calculated and compared with the test result. According to the research, when no balance hole exists, the distribution of liquid velocity in the core area of the hub cavity exhibits axial symmetry, and the circumferential velocity component is approximately 0.4 times of the impeller's rotational speed. When the balance hole exists, the distribution of liquid velocity in the hub cavity does not exhibit axial symmetry, and the circumferential velocity component is larger than 0.4 times of the impeller's rotational speed. The radial leakage velocity on the turbulent boundary layer of the pump cover will increase with the increasing diameter of the balance hole.

Key words: Centrifugal pump, balance hole, hub cavity, circumferential velocity component, radial velocity component

Introduction

The calculations of the axial force and balance of the centrifugal pump have always been hot issues in the pump industry. To open the balance hole on the impeller with the double-sealing ring is one of the widely used methods to balance the axial force of the centrifugal pump^[1-3]. The hub cavity is an area surrounded by the interior wall of the impeller cover, the back sealing ring, the interior wall of the pump cover and the hub. The hub cavity is connected with the balance hole through the impeller inlet, thus, the difference in pressure on both sides of the impeller cover can be reduced to balance the axial force of the impeller. For a long time, researches on the characteristics of flow in the hub cavity have been incomplete and superficial. Semi-theoretical expe-

rience formulas are usually applied to calculate the axial force of the centrifugal pump, which assumes no leakage flow in the cavity on the side of the impeller cover and no rotating flow in the hub cavity^[4-5]. However, these assumptions are inconsistent with the facts. According to Ref. [6], when no balance hole exists, the liquid in the hub cavity rotates together with the impeller because of circumferential force. When the balance hole is opened, flow in the hub cavity is influenced by the rotation of the impeller and leakage flow from the balance hole, and the leakage flow of the balance hole is the main part. According to Ref. [7], the characteristics of flow in the cavity at the impeller cover plate side are closely related to the axial force of the centrifugal pump. According to Refs. [8-9], the characteristics of flow in the cavity at the impeller cover plate side have significant impacts on the performance of the centrifugal pump. The diameter of the balance hole can be obtained through numerical calculation, which has great impact on the axial force of the centrifugal pump^[10]. According to Ref. [11], studies on the characteristics of flow in the cavity at the cover plate side of the centrifugal pump are incomplete for a long term. Thus, to accurately

^{*} Project supported by the National Natural Science Foundation of China (Grant Nos. 51269010, 51236006).

Biography: Wei Dong (1987-), Male, Ph. D., Lecturer

Corresponding author: Wei Dong,

E-mail: dongw@nwfufu.edu.cn

calculate the axial force of the centrifugal pump has been a lasting problem in the pump industry. It is significant to study the influence of the balance hole's diameter on the characteristics of flow in the hub cavity of the centrifugal pump for calculating and balancing axial force of the impeller centrifugal pump.

The grids independence test has been conducted on the designed operating points of the centrifugal pump. The numerical results of flow velocity in the hub cavity have been verified to be consistent with the test results. When the diameter of the impeller balance hole varies within the scope of 0 mm to 12 mm, the flow in the hub cavity is numerically investigated. Then, the influence of the characteristics of flow in the hub cavity on the diameters of the balance holes is analyzed. Besides, the distribution curves for the circumferential and the radial velocity components in the hub cavity along the axial direction and its relationship with the rotational speed of the impeller have also been observed. The leakage rate of the liquid in the hub cavity of the centrifugal pump at the design point is calculated when the diameters of the balance holes are 0 mm, 4 mm, 8 mm and 12 mm. Through comparison with the experimental results on the liquid leakage characteristics in the hub cavity with and without balance holes, the accuracy and feasibility of the numerical results have been validated.

1. Research models

The parameters for this pump are designed as follows: the flow rate, head and efficiency are 200 m³/h, 32 m, and 81%, with a constant rotating speed of 1 450 rpm. The pump has a six-blade impeller and six balance holes. The outer diameter (D), seal ring clearance diameter (b), hub diameter (D_h), front seal ring diameter (D_m), and back seal ring diameter (D_n) of the pump are 325 mm, 0.22 mm, 60 mm, 140 mm and 165 mm. Four diameters of balance holes are selected for this study, i.e., 0 mm, 4 mm, 8 mm and 12 mm, whereby 8 mm is the design value, as shown in Fig. 1.

The same method of grid topology has been applied to different diameter models of the balance holes. The study on grids independence has been widely applied to validate the CFD method^[12-13]. Table 1 shows the result of the grids independence test at the design point of the centrifugal pump.

According to Table 1, the relative errors of efficiency, head and power reached 0.09%, 0.03% and 0.05%, respectively when the total number of grids increased from 1.46×10^6 to 2.34×10^6 . When the grids were further refined, the total number of grids increased from 2.34×10^6 to 3.28×10^6 , and the relative

errors of efficiency, head and power only reached 0.04%, 0.03% and 0%, respectively. Therefore, the simulation reached grid independence when the total number of grids reached 2.34×10^6 . Therefore, the CFD model with the grids of 2.34×10^6 elements was adopted in the numerical study. The grid of impeller and balance holes are shown in Fig. 2.

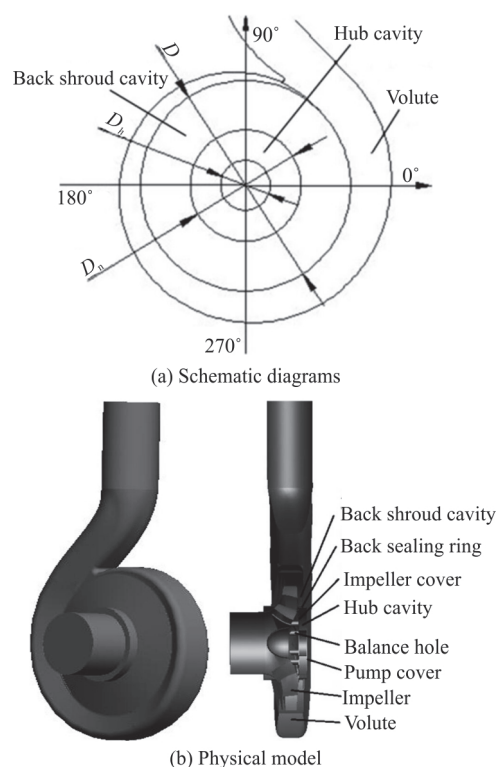


Fig. 1 Computational model

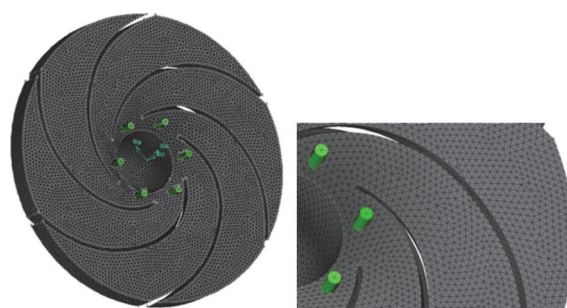


Fig. 2 (Color online) Grid of impeller model

Table 1 Grid independence check

Grid size	Efficiency/%	Head/m	Power/kW
1.46×10^6	81.18	33.07	22.19
2.34×10^6	81.11	33.06	22.20
3.22×10^6	81.14	33.07	22.20

Figure 3 shows the relationship between efficiency (η), head (H) and the diameter of the balance hole at the design point.

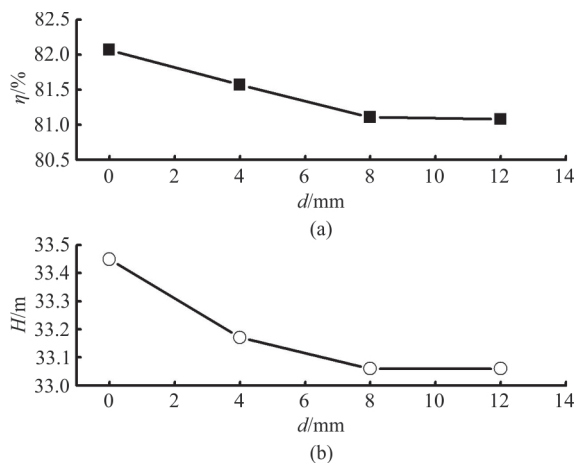


Fig. 3 Calculated results of the pump performance

As shown in Fig. 3, when the diameter of the balance hole increases, the efficiency of the head tends to decline. With a balance hole of $d = 8 \text{ mm}$, the numerical results of the head are higher than the original design parameters of the pump, and the relative error is 3.31%. The numerical results of the efficiency are higher than the original design parameters of the pump, and the relative error is 0.14%. Experiments show that the head and efficiency of a pump decrease with the increase of the balance-hole's diameter. The maximum head and efficiency are achieved when there is no balance hole^[14-15]. The diameter of the balance hole in the impeller changes only for the rest of the three models, the changes of the pump performance are slight, and the numerical results generally approximate to the design parameters. Consequently, the numerical results are reliable, which guarantees the accuracy of the analysis of flow in the pump.

2. Computational methods

Apart from the boundary condition for the outlet, inlet, impeller and volute, grid interfaces among the sealing ring gap, shroud cavity, hub cavity, and balance hole have been created and coupled to be consistent with the actual flow in the pump. Therefore, data of the grid boundary surface in different calculation domains can be completely transferred to form a circular flow in the pump.

(1) Inlet and outlet conditions

The inlet boundary is set as the speed intake, whereas the outlet boundary is set as the free effluent.

(2) Wall conditions

The nonslip solid surface has been set, and the standard wall function method was applied to calculate the turbulent flow near the wall. As shown in Fig. 4, the wall of the pump case was stationary, and

the impeller wall was rotational.

(3) Flow model

The flow in the pump was in compressible and steady, and the RNG $k-\epsilon$ turbulence model was applied.

(4) Control equation and algorithm

The control equation set refers to the continuity and Navier-Stokes equations under the relative coordinate system. The SIMPLEC algorithm is applied to calculate the coupling of pressure and speed.

(5) Discretization

The sub-relaxation item of pressure employed the standard form, whereas the upwind scheme was used for the sub-relaxation items of momentum and turbulence energy and the dissipation rate of turbulence energy in the second order.

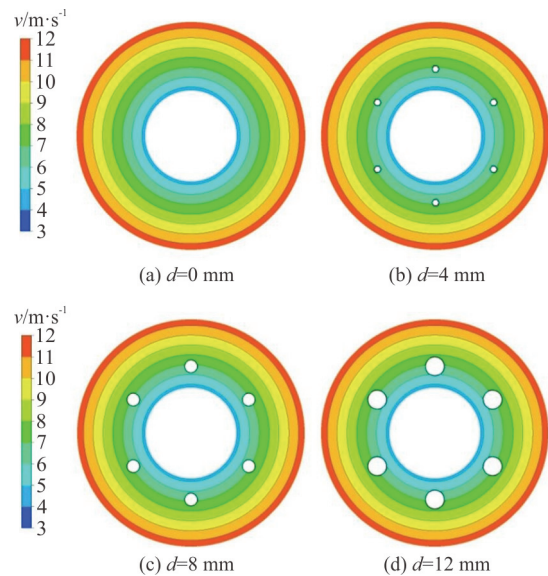


Fig. 4 (Color online) Velocity distribution of the impeller covers in the hub cavity

3. Numerical method validation

The dimensionless tangential velocity \bar{v}_u ($\bar{v}_u = v_u / \omega r$), dimensionless radial velocity \bar{v}_r ($\bar{v}_r = v_r / \omega r$), and dimensionless axial distance coefficient \bar{s} ($\bar{s} = s / \delta$) have been introduced for analysis. v_u refers to the tangential velocity of liquid, v_r refers to the radial speed of liquid, ω refers to the speed of the rotation angle of the impeller, and s refers to the axial distance between the measuring point and the wall of the impeller cover plate. No leakage flow occurs in the hub cavity when there is no balance hole, which approximates the flow of the rotational disk in the enclosed cylinder. According to Ref. [16], the hot-wire anemometer is applied to measure the turbulence speed of the flow field for the rotating disk

in the closed cylinder. As shown in Fig. 5, the test data of the circumferential and the radial velocity components at $0.8R$ are compared with the circumferential and the radial velocity components distributed along the axial direction at $0.8R$ in the hub cavity of the centrifugal pump for the impeller without a balance hole. R refers to the hub cavity semi-diameter.

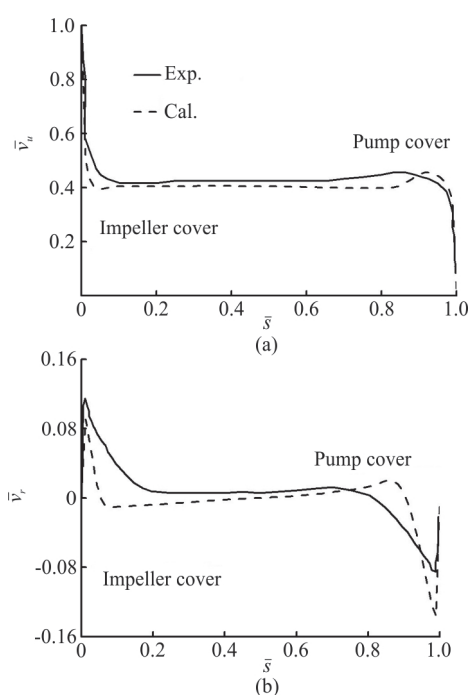


Fig. 5 Comparison of calculation and experimental results

As shown in Fig. 5, the numerical result of the dimensionless circumferential and the radial velocity components distributed along the axial direction for flow in the hub cavity are generally consistent with the test results. A turbulent boundary layer exists near the exterior wall of the impeller cover for the rotational and the interior wall of the stationary pump cover because of liquid viscosity. Moreover, a flow core area exists with a small change along the axial direction between the two boundaries^[17-18]. As a result, the calculation method mentioned in this study can reflect the characteristics of flow in the hub cavity and thus is feasible.

4. Calculation results and analysis

4.1 Absolute velocity in the hub cavity

Figure 6 shows the contours of flow velocity in the geometric center along the axial direction of the hub cavity at the design point when the diameter of the balance hole is 0 mm, 4 mm, 8 mm and 12 mm.

As shown in Fig. 6, when the diameter of the

balance hole increases by 0 mm-12 mm, the changes of the distribution of flow in the hub cavity are complicated. When the diameter is 0 mm (the balance hole doesn't exist), the radial velocity of the liquid in the hub cavity obviously increases from the inner diameter to the outer diameter, with an almost constant circumferential velocity. However, when the diameter is 4 mm, 8 mm and 12 mm, the radial and circumferential velocity of the liquid in the hub cavity is irregular because the gap of the sealing ring and the liquid leakage flow of the balance hole have significantly influenced the flow conditions in the cavity. Stable flow in the radial and circumferential directions cannot form, resulting in a non-uniform distribution of the liquid velocity.

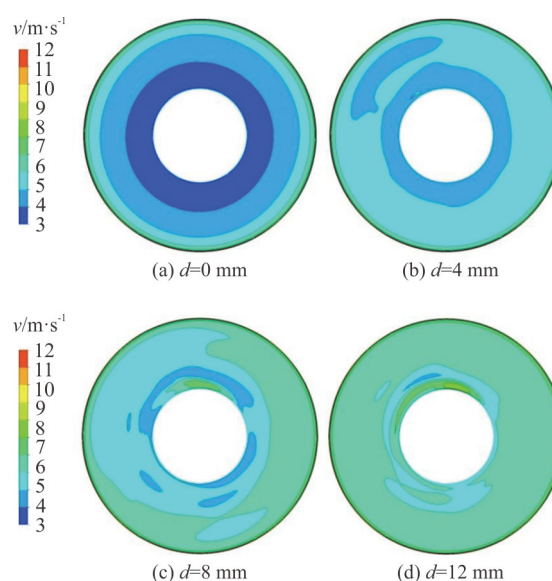


Fig. 6 (Color online) Absolute velocity in the hub cavity

As shown in Fig. 7, when the diameter is 0 mm, there are obviously two boundary layer flows in the hub cavity. Compared with the case without balance hole, the velocity of flow in the hub cavity is significantly increased when the diameter of the balance hole is 4 mm, 8 mm or 12 mm. The liquid in the hub cavity flows through the balance hole to the vane channel and the velocity is found to decrease with the diameter of the balance holes.

4.2 Distribution of velocity in the hub cavity

Moreover, Figures 8, 9 further provide the distribution of the dimensionless circumferential and radial component of the velocity along the axial direction at different radial and circumferential positions when the diameter of the balance hole increases from 0 mm to 12 mm to clarify the influence of the diameter of the balance hole on the characteristics of flow in the hub cavity, and it reflects the specific relationship with the rotational speed of

the impeller. The distribution of flow speed in the hub cavity is further analyzed.

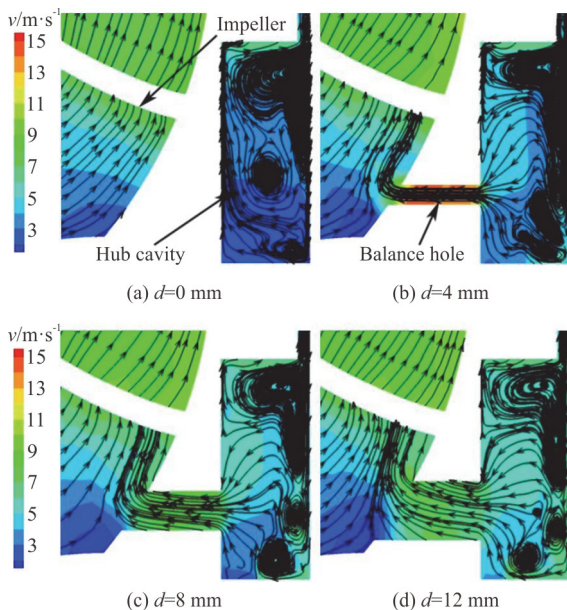


Fig. 7 (Color online) Absolute velocity and limit streamline in the hub cavity

As shown in Fig. 8, when the diameter of the balance hole is 0 mm, the axial distribution of the dimensionless circumferential velocity component with the same circumferential position changes slightly (within the value scope from 0.39 to 0.43) with the radial position. The axial distribution of the dimensionless circumferential velocity at the same radial position is generally equivalent to 0° , 90° , 180° and 270° angles. Therefore, the pressure in the cavity is uniform along the radial direction. There is slight difference in pressure, and it is difficult for the liquid to flow radially in the core area when no balance hole exists. When the diameter of the balance hole equals 4 mm, 8 mm and 12 mm, the axial distribution of the dimensionless circumferential velocity at the same circumferential position tends to decline as the radius increases because the high-energy liquid driven by radial leakage of the sealing ring clearance and rotational wall of the sealing ring transfers the energy from the outer diameter to the inner diameter of the hub cavity. The liquid kinetic energy at the inner diameter increases and the circumferential component of the velocity increases. The axial distribution of the dimensionless circumferential velocity at the same radial position remains the same at 0° , 90° , 180° and 270° angles. It should be noted that the dimensionless circumferential velocity at $0.6R$ of the hub cavity has been most significantly influenced by the axial leakage flow of the liquid from $0.51R$ to $0.67R$, forming an unstable flow along the axial direction.

Whereas the liquid circumferential velocity component at $0.7R$, $0.8R$ and $0.9R$ in the hub cavity is stable along the axial flow, the pressure difference between the rear sealing ring and the balance hole increases when the diameter of the balance hole increases, resulting in significant difference in the distribution of the dimensionless circumferential velocity component for the liquid in the core area along the radial direction. However, the liquid is still distributed by the approximate rotational motion.

Figure 8 also shows the flow within the turbulent boundary layer of the rear cover plate surface in the impeller. Compared with the turbulent core area, the boundary layer region has small axial range. In the core area of the cavity, the rotating impeller results in a high gradient of the circumferential velocity and thus the friction loss of the disk in the impeller surface. The dimensionless circumferential velocity component along the radial and circumferential directions change slightly, exhibiting a certain axial symmetry when the diameter is $d = 0$ mm. When the diameter is $d = 4$ mm, 12 mm and the balance hole is provided at a small radius of $0.6R$, the dimensionless circumferential velocity component is large, at a large radius $0.9R$, the dimensionless circumferential velocity component is small, and no axisymmetric feature is observed. Therefore, the speed difference between the circumferential velocity of the liquid and the rotational speed of the impeller cover plate remains constant in the entire impeller cover plate when the balance hole is not provided. The radial or circumferential friction losses on the impeller disk in the hub cavity are uniform. When the balance hole is provided, the difference between the circumferential velocity of the liquid and the rotational speed of the impeller cover plate increase with the radius, inevitably resulting in the increase in the friction losses on the impeller disk in the hub cavity.

As shown in Fig. 9, under the same balance hole diameter, due to small radius in the hub cavity, the rotational speed of the impeller surface resulting from the centrifugal force is small (the rotational speed for the outer radius of the impeller is approximately 25.2 m/s, and the rotational speed for the impeller cover plate in the hub cavity is lower than 12 m/s) and the pump cover is stationary, resulting in the small fluctuation of the dimensionless radial velocity component near the exterior surface of the impeller cover plate and the area with dimensionless radial velocity component lower than zero near the inner surface of the pump cover. However, under the radii $0.6R$, $0.7R$, $0.8R$ and $0.9R$ with the same angle or under the angles 0° , 90° , 180° and 270° and the same radius, the dimensionless radius speed for liquid in the core area changes slightly and is approximate to zero. As a result, due to the difference of radial pres-

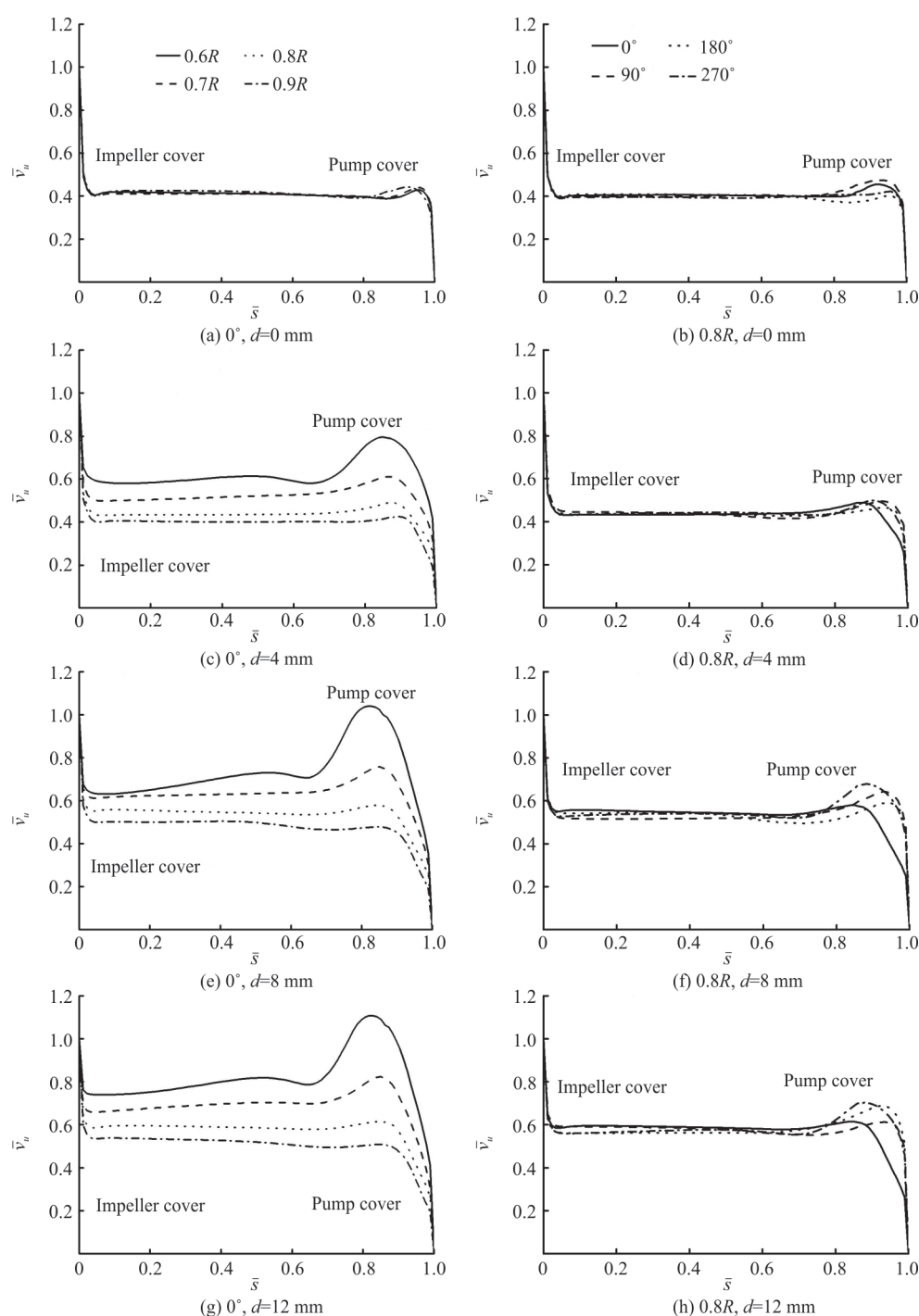


Fig. 8 Axial distribution of dimensionless circumferential velocity component in the hub cavity

sure, radial leakage flow occurs for the liquid in the hub cavity. The leakage mainly occurs near the boundary layer of the pump cover surface, and no radial flow exists for liquid in the core area. When the diameter is $d = 4$ mm, 8 mm and 12 mm and the balance hole is provided, the balance hole area of the impeller $0.51R$ to $0.67R$, resulting in a large fluctuation of the dimensionless radial velocity component for $0.6R$ liquid in the hub cavity.

As shown in Fig. 9, when the diameter is $d = 0$ mm, due to the small radial pressure difference in the hub cavity, the dimensionless radial component of the velocity of the liquid in the hub cavity changes slightly in the turbulent boundary layer with the angle and radius, resulting in a small radial leakage flow. When the diameter is $d = 4$ mm, 8 mm and 12 mm, the dimensionless radial velocity component of the liquid in the hub cavity changes significantly with the

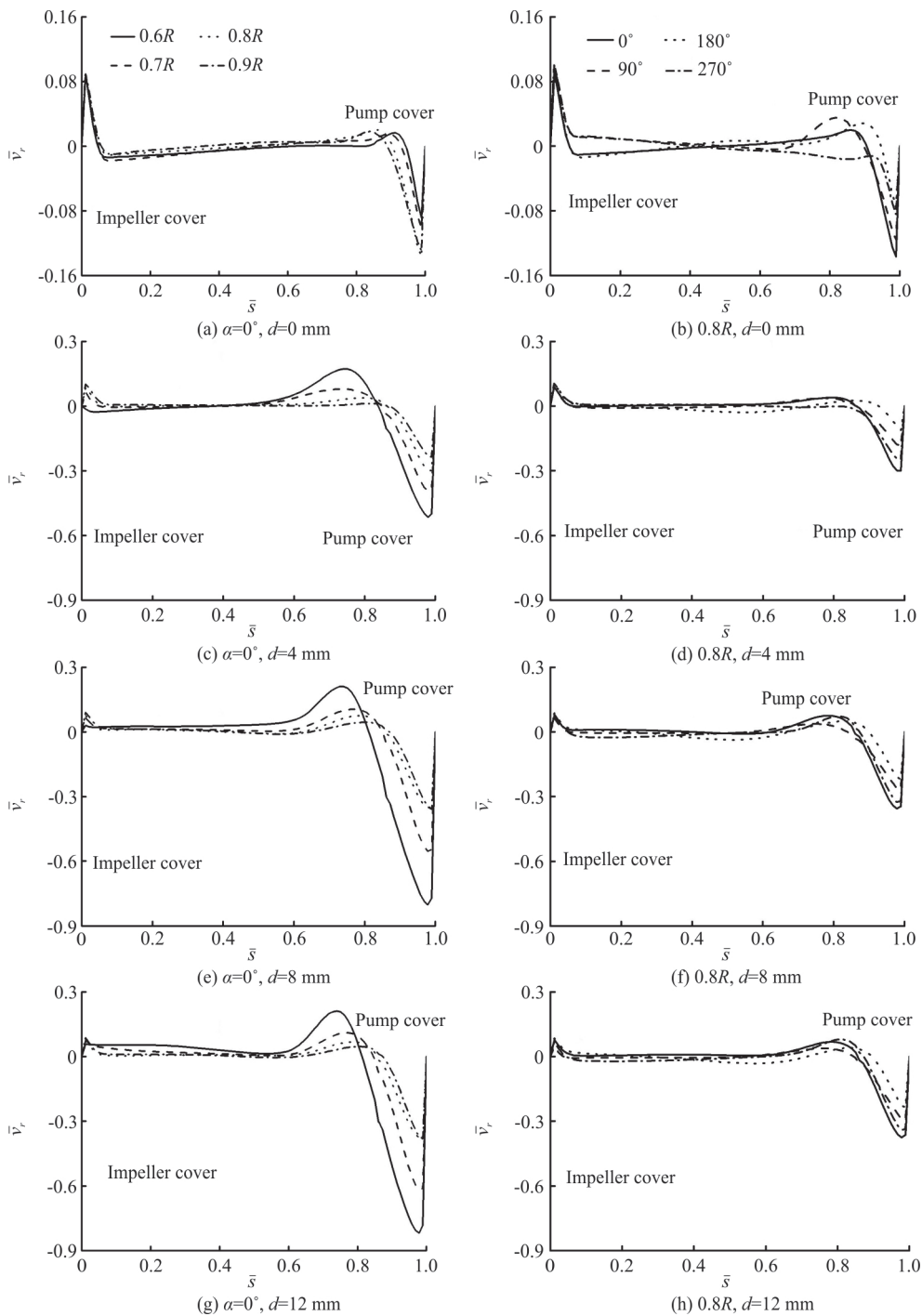


Fig. 9 Axial distribution of dimensionless radial velocity component in the hub cavity

angle and radius in the turbulent boundary layer. Stable flow cannot form in the cavity because of the liquid leakage flow in the sealing ring gap and balance hole, resulting in a non-uniform radial velocity for the liquid in the cavity. When the diameter of the balance hole increases from 0 mm to 12 mm, the area with dimensionless radial velocity component lower than zero increases at the turbulent boundary layer near the pump cover surface in the hub cavity, especially for

the region at the angle of 0°. As a result, when the diameter of the balance hole as well as the radial pressure difference increase, the radial leakage speed in the hub cavity and the leakage amount increase.

It is known from previously presented analysis that when the diameter of the balance hole is changed, the flow in the hub cavity is always 2-D circumferential shear flow with radial pressure difference. When the balance hole is provided, the axial leakage

of the balance hole significantly influence the characteristics of flow in the hub cavity, which is consistent with the results in Ref. [6], i.e., when the diameter is 8 mm and the balance hole is provided, flow in the hub cavity is induced by the rotating impeller and leakage flow of the balance hole, and the leakage flow of the balance hole is the main part. Thus, the research results are consistent with the actual flow conditions in the pump with high reliability.

4.3 Numerical analysis and verification of leakage amount

Because of the higher pressure in the rear pump cavity compared with in the hub cavity, the liquid in the rear pump cavity leaks from the rear sealing ring clearance into the hub cavity and then into the inlet of the impeller through the balance hole. Many studies indicate that liquid leakage in the sealing ring clearance can verify the distribution of the flow speed in the cavity^[19-20]. In Ref. [6], the leakage in the hub cavity of the centrifugal pump has been tested on a closed test bed of the water pump with or without balance hole. The mass flow rate of the leakage flow in the rear sealing ring gap of the centrifugal pump is calculated through the pressure measured at radius $r_1 = 110$ mm in the pump cavity and radius $r_2 = 62$ mm in the hub cavity according to the theoretical formula. The YB-150 standard pressure meter is used to measure the pressure in the back shroud cavity and hub cavity, and the LWGY-DN150 intelligent turbine flowmeter is used to measure the flow and indicate the real-time flow. The measurement error is lower than 0.5%. Figure 10 shows the method of measuring pressure.

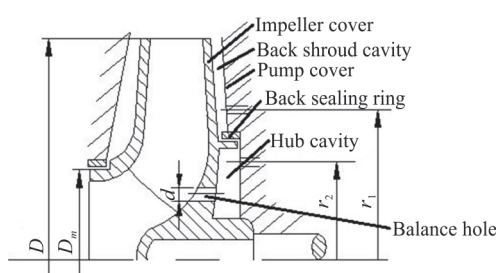


Fig. 10 Sketch of pressure test on the cavities

Fluid leakage q_v in the back sealing ring is as follows^[6]

$$q_v = \psi D_m \pi b \sqrt{2g\Delta H} \quad (1)$$

Flow coefficient ψ in the sealing ring is as follows

$$\psi = \frac{1}{\sqrt{1 + 0.5\xi + \frac{\lambda L}{2b}}} \quad (2)$$

The fore-and-aft pressure difference (ΔH) in the back sealing ring is as follows

$$\Delta H = \frac{p_1}{\rho g} - \frac{p_2}{\rho g} \quad (3)$$

where $p_1/\rho g$ is the measured value at radius r_1 of the shroud cavity, $p_2/\rho g$ is the measured value at radius r_2 of the hub cavity, ξ is the shape coefficient and λ is the resistance coefficient.

Figure 11 gives the test and numerical results at the design operating points.

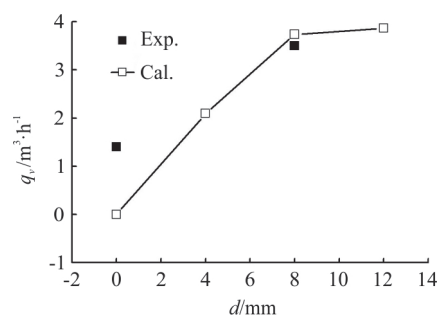


Fig. 11 Comparison of the liquid leakage amount

Due to the change of axial force across the impeller, when the balance hole diameter increases from 0 mm to 8 mm, the impeller will move slightly along the axial direction and therefore alters the leakage flow because of the change of the axial clearance between the impeller and the pump cover^[17]. However, in the simulation, the impeller of the centrifugal pump has a fixed axial position and the axial clearance remains the same with and without the balance hole. The hub cavity is similar to a closed cylinder when no balance hole exists and the leakage amount tends to be zero. Therefore, the numerical results of the leakage in the hub cavity are lower than the test results. As shown in Fig. 10, the comparison between balance hole of $d = 8$ mm and $d = 0$ mm indicates an obvious increase of leakage flow in both the test results and the numerical results, with a consistent trend. When $d = 8$ mm, the numerical results for the liquid leakage in the hub cavity are generally consistent with the test results. Therefore, the numerical calculation results for the leakage rate of the liquid in the hub cavity are accurate and reliable,

which also indicates highly reliable research results.

5. Conclusions

(1) The flow in the hub cavity approximates the flow in a closed cylinder when no balance hole exists. The distribution of the liquid speed in the core area exhibits axial symmetry, whereas the circumferential velocity component is approximately 0.4 times of the rotational speed of the impeller and the radial velocity component is approximately zero.

(2) Flow in the hub cavity will be significantly influenced by the radial leakage of the turbulent boundary layer of the pump cover and the axial leakage of the balance hole when no balance hole exists. Therefore, the distribution of liquid speed does not exhibit axial symmetry. The circumferential velocity component for liquid in the core area is 0.4 times larger than that of the rotational speed of the impeller. Radial leakage mainly occurs around the cover pump wall.

(3) A larger diameter of the balance hole results in a higher radial leakage speed on the turbulent boundary layer of the pump cover wall and a higher liquid leakage amount in the rear sealing ring gap of the centrifugal pump.

Acknowledgements

This work was supported by the Fundamental Research Funds for the Central Universities (Grant No. Z1090219041), the Science and Technology Plan Project Funds for Shaanxi Provincial Department of Water Resources (Grant No. 2019slkj-15) and the Basic Natural Science Research Program of Shaanxi Province (Grant No. 2019JLM-58).

References

- [1] Cao W., Dai X., Hu Q. Effect of impeller reflux balance holes on pressure and axial force of centrifugal pump [J]. *Journal of Central South University*, 2015, 22(5): 1695-1706.
- [2] Babayigit O., Ozgoren M., Aksoy M. H. et al. Experimental and CFD investigation of a multistage centrifugal pump including leakages and balance holes [J]. *Desalination and Water Treatment*, 2017, 67(5): 28-40.
- [3] Wu D. Z., Yang S., Xu B. J. et al. Investigation of CFD calculation method of a centrifugal pump with unshrouded impeller [J]. *Chinese Journal of Mechanical Engineering*, 2014, 27(2): 376-384.
- [4] Xia B., Kong F., Zhang H. et al. Investigation of axial thrust deviation between the theory and experiment for high-speed mine submersible pump [J]. *Advances in Mechanical Engineering*, 2018, 10(8): 1-13.
- [5] Dong W., Chu W. L. Numerical investigation of the fluid flow characteristics in the hub plate crown of a centrifugal pump [J]. *Chinese Journal of Mechanical Engineering*, 2018, 31(1): 1-10.
- [6] Liu Z. L., He R., Fan Y. Fluid leakage characteristics test on the balance cavity of floating impeller [J]. *Transactions of the Chinese Society for Agricultural Machinery*, 2011, 42(9): 113-115(in Chinese).
- [7] Mortazavi F., Riasi A., Nourbakhsh A. Numerical investigation of back vane design and its impact on pump performance [J]. *Journal of Fluids Engineering*, 2017, 139(12): 121104.
- [8] Will B. C., Benra F. K., Dohmen H. J. Investigation of the flow in the impeller side clearances of a centrifugal pump with volute casing [J]. *Journal of Thermal Science*, 2012, 21(3): 197-208.
- [9] Ayad A. F., Abdalla H. M., Aly A. A. E. A. Effect of semi-open impeller side clearance on the centrifugal pump performance using CFD [J]. *Aerospace Science and Technology*, 2015, 47(12): 247-255.
- [10] Zhang L. S., Jiang J., Xiao Z. H. et al. Numerical investigation of the effect of balancing-hole on the axial force of a partial emission pump [C]. *Proceedings of the ASME 2014 4th Joint US-European Fluids Engineering Division Summer Meeting (FEDSM2014-21418)*, Chicago, Illinois, USA, 2014, 1-6.
- [11] Dong W., Chu W. L. Numerical study of flow characteristics and disc friction loss in the balance cavity of centrifugal pump impeller [J]. *Transactions of the Chinese Society for Agricultural Machinery*, 2016, 47(4): 29-35(in Chinese).
- [12] Liu H., Wang K., Yuan S. et al. Multicondition optimization and experimental measurements of a double-blade centrifugal pump impeller [J]. *Journal of Fluid Engineering*, 2013, 135(1): 011103.
- [13] Li W., Jiang X., Pang Q. et al. Numerical simulation and performance analysis of a four-stage centrifugal pump [J]. *Advances in Mechanical Engineering*, 2016, 8(10): 1-8.
- [14] Liu Z. L., Shi F. X., Wang R. Z. et al. Influence of impeller balancing hole diameter on hydraulic performance of centrifugal pump [J]. *Journal of Lanzhou University of Technology*, 2016, 42(6): 57-61(in Chinese).
- [15] Dong W., Chu W. L. Influence of balance hole diameter on performance and balance chamber pressure of centrifugal pump [J]. *Transactions of the Chinese Society for Agricultural Machinery*, 2015, 46(6): 73-77(in Chinese).
- [16] Itoh M., Yamada Y., Imao S. et al. Experiments on turbulent flow due to an enclosed rotating disk [J]. *Experimental Thermal and Fluid Science*, 1992, 5(3): 359-368.
- [17] Hu X. Q., Wang X. Y., Lei X. C. et al. Numerical investigations of the effects of blade shape on the flow characteristics in a stirred dead-end membrane bioreactor [J]. *Journal of Hydrodynamics*, 2018, 30(6): 1143-1152.
- [18] Takamine T., Furukawa D., Watanabe S. et al. Experimental analysis of diffuser rotating stall in a three-stage centrifugal pump [J]. *International Journal of Fluid Machinery and Systems*, 2018, 11(1): 77-84.
- [19] Daqiqshirazi M., Torabi R., Riasi A. et al. The effect of wear ring clearance on flow field in the impeller sidewall gap and efficiency of a low specific speed centrifugal pump [J]. *Proceedings of the Institution of Mechanical Engineers Part C-Journal of Mechanical Engineering Science*, 2018, 232(17): 3062-3073.
- [20] Kye B., Park K., Choi H. et al. Flow characteristics in a volute-type centrifugal pump using large eddy simulation [J]. *International Journal of Heat and Fluid Flow*, 2018, 72: 52-60.